Measurements of cross sections for the fusion-evaporation reactions ^{244}Pu(^{48}Ca,xn)$^{292-x}$114 and ^{245}Cm(^{48}Ca,xn)$^{293-x}$116

Yu. Ts. Oganessian, V. K. Utyonkov, Yu. V. Lobanov, F. Sh. Abdullin, A. N. Polyakov, I. V. Shirokovsky, Yu. S. Tsyganov, G. G. Gulbekian, S. L. Bogomolov, B. N. Gikal, A. N. Mezentsev, S. Iliev, V. G. Subbotin, A. M. Sukhov, A. A. Voinov, G. V. Buklanov, K. Subotic, V. I. Zagrebaev, and M. G. Itkis
Joint Institute for Nuclear Research, 141980 Dubna, Russian Federation

J. B. Patin, K. J. Moody, J. F. Wild, M. A. Stoyer, N. J. Stoyer, D. A. Shaughnessy, J. M. Kenneally, and R. W. Lougheed
University of California, Lawrence Livermore National Laboratory, Livermore, California 94551, USA
(Received 1 December 2003; published 17 May 2004)

We have studied the excitation functions of the reactions ^{244}Pu(^{48}Ca,xn). Maximum cross sections for the evaporation of 3–5 neutrons in the complete-fusion reaction ^{244}Pu+^{48}Ca were measured to be $\sigma_{3n}=2$ pb, $\sigma_{4n}=5$ pb, and $\sigma_{5n}=1$ pb. The decay properties of 3n-evaporation product ^{289}114, in the decay chains observed at low ^{48}Ca energy coincide well with those previously observed in the ^{244}Pu+^{48}Ca and ^{248}Cm+^{48}Ca reactions and assigned to ^{288}114. Two isotopes of element 114 and their descendant nuclei were identified for the first time at higher bombarding energies: ^{288}114 ($E_\alpha=9.95$ MeV, $T_{1/2}=0.6$ s) and ^{287}114 ($E_\alpha=10.04$ MeV, $T_{1/2}=1$ s). We also report on the observation of new isotopes of element 116, ^{290,291}116, produced in the ^{245}Cm + ^{48}Ca reaction with cross sections of about 1 pb. A discussion of self-consistent interpretations of all observed decay chains originating at $Z=118$, 116, and 114 is presented.

DOI: 10.1103/PhysRevC.69.054607 PACS number(s): 25.70.Gh, 23.60.+e, 25.85.Ca, 27.90.+b

I. INTRODUCTION

In previous experiments in which superheavy nuclei close to the predicted neutron magic number $N=184$ were synthesized, we used the complete-fusion reactions of target and projectile nuclei having the largest available neutron excess: ^{244}Pu+^{48}Ca [1], ^{248}Cm+^{48}Ca [2], and ^{249}Cf+^{48}Ca [3]. In all of these cases, the observed α-decay chains of parent isotopes of elements 114, 116, and 118 were terminated by the spontaneous fission (SF) of previously unknown descendant nuclei with $Z=110$ [1,2] or 114 [3]. Because of the lack of available target and projectile reaction combinations, these unknown descendant nuclei cannot be produced as a primary reaction product. Thus the method of genetic correlations to known nuclei for the identification of the parent nuclide (see, e.g., review [4] and references therein) has limited application in this region of nuclei.

In these experiments, we identified masses of evaporation residues (ER's) using the characteristic dependence of their production cross sections on the excitation energy of the compound nucleus (thus defining the number of emitted neutrons) and from cross bombardments, i.e., varying mass number of the projectile or target nuclei which changes the relative yields of the xn-evaporation channels. Both of these methods were successfully used in previous experiments for the identification of unknown artificial nuclei (see [5] and references therein), particularly those with short half-lives for decay by SF.

We present the results of excitation-function measurements for the ^{244}Pu+^{48}Ca fusion-evaporation reactions. We also report on the synthesis of new isotopes of element 116 in the ^{245}Cm+^{48}Ca reaction.

II. EXPERIMENTAL TECHNIQUE

The ^{48}Ca ion beam was accelerated by the U400 cyclotron at the Flerov Laboratory of Nuclear Reactions (FLNR). The typical beam intensity at the target was 1.2 pμA. The 32-cm^2 rotating targets consisted of the enriched isotopes ^{244}Pu (98.6%) and ^{245}Cm (98.7%) deposited as PuO_2 and CmO_2 onto 1.5-μm Ti foils to thicknesses of about 0.38 mg cm^{-2} and 0.35 mg cm^{-2}, respectively.

The ER's recoiling from the target were separated in flight from ^{48}Ca beam ions, scattered particles and transfer-reaction products by the Dubna Gas-filled Recoil Separator [6]. The transmission efficiency of the separator for $Z=114$ and 116 nuclei was estimated to be about 35–40% [6]; the separator efficiency is slowly changing as a function of mass and recoil energy over the range studied in these experiments.

Evaporation recoils passed through a time-of-flight system (TOF) and were implanted in a 4×12 cm^2 semiconductor detector array with 12 vertical position-sensitive strips, located in the separator's focal plane. This detector was surrounded by eight 4×4 cm^2 side detectors without position sensitivity, forming a box of detectors open from the front (beam) side. The position-averaged detection efficiency for α-decays of implanted nuclei was 87% of 4π. The detection system was tested by registering the recoil nuclei and decays (α or SF) of the known isotopes of No and Th, as well as their descendants, produced in the reactions ^{206}Pb(^{48}Ca,xn) and ^{nat}Yb(^{48}Ca,xn). The energy resolution for α particles absorbed in the focal-plane detector was 60–90 keV. The α-particles that escaped the focal-plane detector at different angles and registered in a side detector had an energy resolution of the summed signals of 140–200 keV. The FWHM position resolutions of the signals of correlated decays of

TABLE I. Reaction-specific lab-frame beam energies in the middle of the target layers, excitation energies [7] and beam doses for the given reactions.

Reaction	E_{beam} MeV	E^* MeV	Beam dose	Reference
^{244}Pu+^{48}Ca	231	29.8–32.9	4.6×10^{18}	[1]
	236	32.9–37.4	1.5×10^{19}	[1]
	243	38.9–43.0	4.0×10^{18}	this work
	250	44.9–49.0	3.1×10^{18}	this work
	257	50.4–54.7	2.9×10^{18}	this work
^{245}Cm+^{48}Ca	243	30.9–35.0	1.2×10^{19}	this work

nuclei implanted in the detectors were 0.8–1.3 mm for ER-α signals and 0.5–0.8 mm for ER-SF signals. As it can be seen from the data presented below, all the correlated events observed in these experiments were registered with position deviations corresponding to the given position resolutions except for two SF events. However, both these SF events were detected in beam-off period and the probability of observing them as random events is negligibly low. Fission fragments from ^{252}No implants produced in the ^{206}Pb+^{48}Ca reaction were used for an approximate fission-energy calibration. The measured fragment energies were not corrected for the pulse-height defect of the detectors, or for energy loss in the detectors' entrance windows, dead layers, and the pentane gas filling the detection system. The mean sum energy loss of fission fragments from the decay of ^{252}No was about 20 MeV.

III. RESULTS

A. Excitation functions of ER's produced in ^{244}Pu+^{48}Ca reaction

In this series of experiments, we chose bombarding energies for the ^{48}Ca ions that were greater than what had been studied previously [1]. Table I summarizes the lab-frame beam energies in the middle of the target layers, excitation energy ranges [7] and beam doses for the experiments studied. The systematic uncertainty in the beam energy is about 1 MeV. With the beam energy resolution, the small variation of the beam energy during irradiation, and the energy loss in the target, we expected the resulting compound nucleus ^{292}114 to have excitation-energy ranges of 3.1 to 4.5 MeV. In our previous experiments performed in the years 1998–1999 [1], a ^{244}Pu target was bombarded with a similar beam dose at lower excitation energies (see Table I).

To detect these decay sequences in low background conditions, we employed a special measurement mode [2,3]. The beam was switched off after a recoil signal was detected with parameters of implantation energy and TOF expected for $Z=114$ evaporation residues, followed by an α-like signal with an energy of 9.66 MeV$\leqslant E_\alpha \leqslant$10.08 MeV, in the same strip, within a 1.4–1.9 mm wide position window and a time interval of 10 s. The duration of the pause was determined from the observed pattern of out-of-beam α decays and varied from 3 to 12 min. Thus, all the expected sequential decays of the daughter nuclides with $Z\leqslant112$ should be observed in the absence of beam-associated background.

The measured parameters of the decay chains observed at the three bombarding energies, namely detected energies of events E, positions of the ER's with respect to the top of the strip P_{ER}, difference in vertical positions relative to the ER δP, time intervals δt between detected events, and strip numbers are shown in Table II. At 243 MeV, we observed two decay chains (see the first two rows of Table II), each consisting of two consecutive α decays terminated by SF. The assignment of the event with $E_\alpha=9.9\pm0.9$ MeV to the ^{289}114 in the second decay chain is rather tentative because its registration probability in 6.3 s time interval as a random signal is about 40% (average counting rate of such events by the whole side detector array was about 4.5 min^{-1}). The same values for three other similar events (rows 3, 5, and 12) are about 18%, 2%, and 6%, respectively. However, the detection probability of this chain (ER-α_2-SF) caused by unrelated signals is quite low $P_{\mathrm{err}}<5\times10^{-4}$. The assignment of the side-only α decay of ^{289}114 for rows 2 and 3 is not as strong as a chain with a full energy alpha signal, but it cannot be excluded. Identical decay chains were previously identified in the same reaction at the lower energy of 236 MeV (two events) [1] and also detected after the α decay of the parent nuclei in the ^{248}Cm+^{48}Ca reaction (three events) [2]. One more event of this type was detected at 250 MeV. At 257 MeV, no such events were found. Thus, this activity was observed in the ^{48}Ca energy interval of 236–250 MeV ($E^*=35-47$ MeV). The time intervals between the implantation of the mother nuclei in the detectors and the SF of the granddaughter isotopes varied from one-half minute to three minutes.

In addition to these chains at 243 MeV, we found seven similar decay chains that did not resemble those previously observed in the ^{244}Pu+^{48}Ca and ^{248}Cm+^{48}Ca reactions at lower compound nucleus excitation energies [1,2]. These decay chains consisted of a single α decay followed by the SF decay of the daughter nucleus, both detected within one second of the ER implantation. Four more decay chains of this type were observed at 250 MeV and one additional chain was observed at 257 MeV. These nuclei were also observed in the narrow energy interval of 243–257 MeV ($E^*=41-53$ MeV).

All of the events of this type of decay, observed at the various ^{48}Ca energies, are presented in the second section of Table II. The parent nuclei in these chains emit an α particle with an energy of 9.95 MeV in a short time following the ER implantation ($T_\alpha\sim0.6$ s). The daughter nuclei undergo SF decay with a half-life of $\sim$0.1 s.

The excitation functions for producing various nuclei in the ^{244}Pu+^{48}Ca are shown in Fig. 1. They correspond well with what we expect for the indicated xn-evaporation channels [5]. As one can see from Fig. 1, the excitation functions of the nuclei that undergo sequential decays (α-α-SF and α-SF), overlap and their maxima are located at $E^*\sim40-43$ MeV. The spectra of α particles and pairs of SF fragments observed in these chains are given in Fig. 2 together with the data from the reaction ^{248}Cm+^{48}Ca [2]. In both cases, the radioactive decay of the observed nuclei is characterized by a strictly defined α-transition energy. The

TABLE II. Observed decay chains produced in the described reactions. Bolded events were registered in beam-off period. The α-particle energy errors are shown in parentheses.

$^{244}Pu + ^{48}Ca$

		$^{289}114$			$^{289}114$			$^{285}112$			$^{281}110$	
Strip	E_L (MeV)	E_{ER} (MeV)	P_{ER} (mm)	$\delta t_{ER-\alpha}$ (s)	E_α (MeV)	$\delta P_{ER-\alpha}$ (mm)	$\delta t_{\alpha-\alpha}$ (s)	E_α (MeV)	$\delta P_{ER-\alpha}$ (mm)	$\delta t_{\alpha-SF}$ (s)	E_{SF} (MeV)	δP_{ER-SF} (mm)
12	243	6.1	26.2	0.112	9.80(7)	−0.7	14.80	**9.16(7)**	−1.0	9.892	**133**	−0.5
1	243	9.4	19.1	6.292	9.9(6)[a]		27.94	9.17(7)	+1.2	40.91	202[d]	−0.7
8	250	9.0	24.3	5.718	9.9(3)[a]		20.61	9.18(8)	+0.6	4.679	138	−0.1
		$^{288}114$			$^{288}114$			$^{284}112$				
Strip	E_L (MeV)	E_{ER} (MeV)	P_{ER} (mm)	$\delta t_{ER-\alpha}$ (s)	E_α (MeV)	$\delta P_{ER-\alpha}$ (mm)	$\delta t_{\alpha-SF}$ (s)	E_{SF} (MeV)	δP_{ER-SF} (mm)			
11	243	7.7	17.1	0.826	9.98(8)	+0.3	0.177	229	0.0			
5	243	11.9	11.3	0.838	2.9[b]		0.168	225[d]	−0.1			
2	243	9.8	21.8		(missing α)		0.565	191	−0.2			
4	243	12.2	18.5	0.378	10.02(7)	+0.2	0.326	**137**	−0.5			
4	243	11.5	20.7	0.427	9.97(7)	+0.7	0.072	**230**[d]	−0.1			
6	243	7.4	36.4	0.676	9.91(9)	+0.7	0.007	**150**	+0.2			
5	243	11.5	34.4	0.083	9.92(8)	+0.1	0.028	**221**	+0.6			
2	250	12.1	28.2	0.188	9.93(8)	+0.7	0.130	**205**[d]	+0.1			
4	250	11.8	21.1	0.930	9.9(6)[a]		0.069	155	−0.6			
3	250	11.2	26.6	0.391	9.94(7)	+0.2	0.389	**221**[d]	−0.3			
7	250	11.7	29.5	0.823	9.87(9)	+0.4	0.063	**194**	−1.8			
2	257	11.0	21.2	4.468	10.05(19)[c]		0.123	199[d]	+0.1			
		$^{287}114$			$^{287}114$			$^{283}112$			$^{279}110$	
Strip	E_L (MeV)	E_{ER} (MeV)	P_{ER} (mm)	$\delta t_{ER-\alpha}$ (s)	E_α (MeV)	$\delta P_{ER-\alpha}$ (mm)	$\delta t_{\alpha-\alpha}$ (s)	E_α (MeV)	$\delta P_{ER-\alpha}$ (mm)	$\delta t_{\alpha-SF}$ (s)	E_{SF} (MeV)	δP_{ER-SF} (mm)
3	257	12.4	17.6	1.499	10.03(7)	+0.6	5.457	**9.54(7)**	+0.6	0.319	**206**[d]	0.0

$^{245}Cm + ^{48}Ca$

		$^{291}116$			$^{291}116$			$^{287}114$			$^{283}112$			$^{279}110$	
Strip	E_L (MeV)	E_{ER} (MeV)	P_{ER} (mm)	$\delta t_{ER-\alpha}$ (ms)	E_α (MeV)	$\delta P_{ER-\alpha}$ (mm)	$\delta t_{\alpha-\alpha}$ (s)	E_α (MeV)	$\delta P_{ER-\alpha}$ (mm)	$\delta t_{\alpha-\alpha}$ (s)	E_α (MeV)	$\delta P_{ER-\alpha}$ (mm)	$\delta t_{\alpha-SF}$ (s)	E_{SF} (MeV)	δP_{ER-SF} (mm)
3	243	13.2	36.4	6.02	10.75(31)[a]		0.898	10.08(7)	0.0	12.57	**9.55(7)**	−0.3	0.687	**205**[d]	+0.1
1	243	13.4	23.5	12.3	10.74(7)	−0.1	2.273	**10.01(7)**	0.0	8.303	**9.52(7)**	−0.3	0.256	**177**	−2.2
		$^{290}116$			$^{290}116$			$^{286}114$			$^{282}112$				
Strip	E_L (MeV)	E_{ER} (MeV)	P_{ER} (mm)	$\delta t_{ER-\alpha}$ (ms)	E_α (MeV)	$\delta P_{ER-\alpha}$ (mm)	$\delta t_{\alpha-\alpha/SF}$ (ms)	$E_{\alpha/SF}$ (MeV)	$\delta P_{ER-\alpha/SF}$ (mm)	$\delta t_{\alpha-SF}$ (ms)	E_{SF} (MeV)	δP_{ER-SF} (mm)			
2	243	12.7	30.5	0.233	10.88(8)	−0.9	328	193[d]	−0.5						
2	243	15.6	32.3		(missing α)		914	176	−0.1						
2	243	11.9	25.5		(missing α)		505	10.03(31)[a]		1.448	169	−0.6			

[a]Escaped α particle registered by side detector only.

[b]Escaped α particle registered by focal-plane detector without position signal because of low energy deposited.

[c]α particle registered by both focal-plane detector and side detector.

[d]Fission event registered by both focal-plane detector and side detector.

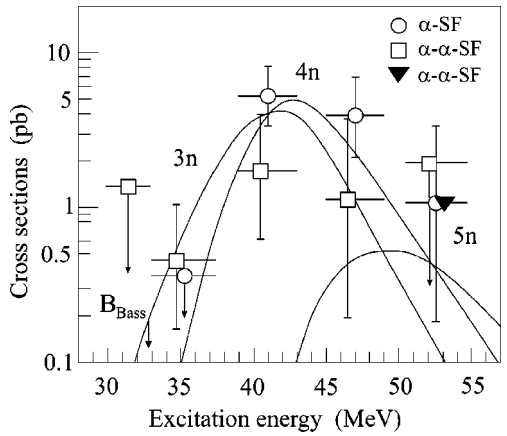

FIG. 1. Excitation functions for the $3n$ (□), $4n$ (○), and $5n$ (▼) evaporation channels from the complete-fusion reaction ^{244}Pu $+^{48}$Ca. The Bass barrier [8] is shown by an arrow. Lines show the results of calculations [9]. Error bars correspond to statistical uncertainties.

relationship of the decay energy, Q_α, and the half-life, T_α, for $Z=114$ gives evidence for the observation of unhindered α transitions that are typical for the decay of even-even nuclides (see Table III). Decay energies of the mother nuclei in these two cases differ by only 0.1 MeV. If we consider only the decay properties of the $Z=114$ species themselves, there is insufficient evidence to identify more than one nuclide from the experimental data.

However, the decay properties of the daughter nuclei differ considerably. In the longer chains (α-α-SF), the daughter nucleus undergoes α decay in all 8 cases with $T_\alpha=34^{+17}_{-9}$s. In the shorter chains (α-SF), the daughter nucleus decays in all 12 cases by spontaneous fission with $T_{SF}=0.098^{+0.041}_{-0.023}$s. This difference in T_α and T_{SF} lies far beyond statistical uncertainties and can only be explained by the fact that the two observed types of decay chains originate from two neighboring isotopes of element 114 if one does not assume SF decays from isomeric states.

Finally, at the maximum beam energy of 257 MeV, we detected a single example of a new type of decay chain, not observed at lower energies. This chain includes two sequential α particles with energies of 10.03 MeV and 9.54 MeV and ends in SF, with all decays detected in a time interval of about ten seconds (see the third section of Table II and Fig. 1).

Although the α decay energy of the mother nucleus in this new decay chain is similar to those observed in the two previously considered chains (a difference of ~0.2 MeV and ~0.1 MeV, respectively), the daughter nucleus in this chain differs in decay energy as well as in half-life. Assuming that this chain belongs to the decay of another new nucleus, we arrive at the conclusion that in the present ^{244}Pu+^{48}Ca ex-

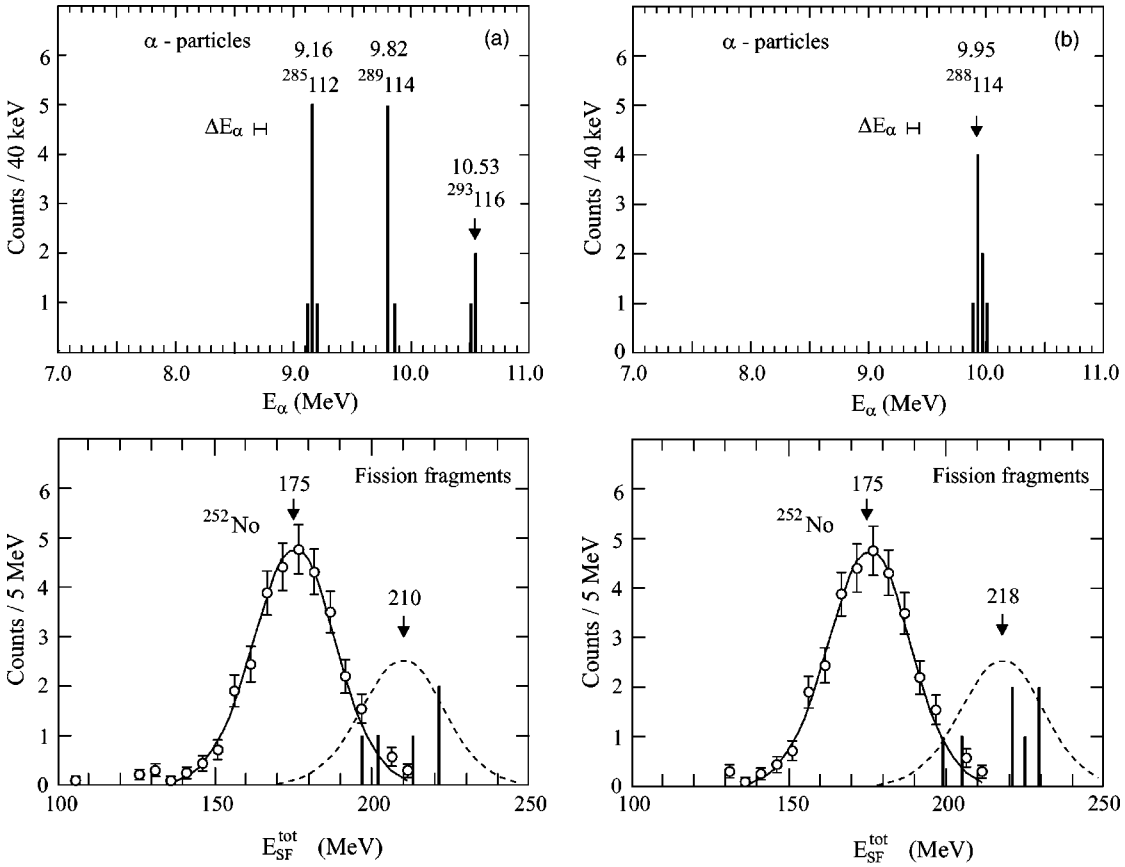

FIG. 2. α-particle (top panel) and sum fission-fragment (bottom panel) energy spectra of events in correlated decay chains originating from parent nuclei ^{293}116 (α energies from [2]), ^{289}114 (a) and ^{288}114 (b). The sum fission-fragment energy spectrum of ^{252}No is shown for comparison. In the top panel, the α-particle energy resolution is shown by ΔE_α.

TABLE III. Decay properties of nuclei produced in this work and [1–3].

Isotope	No. observed	Decay mode	Half-life	Expected half-life	E_α (MeV)
$^{293}116$	3	α	53^{+62}_{-19}ms	80 ms	10.53±0.06
$^{289}114$	8	α	$2.7^{+1.4}_{-0.7}$s	2 s	9.82±0.06
$^{285}112$	8	α	34^{+17}_{-9}s	50 s	9.16±0.06
$^{281}110$	8	SF	$9.6^{+5.0}_{-2.5}$s		
$^{288}114$	11	α	$0.63^{+0.27}_{-0.14}$s	0.8 s	9.95±0.08
$^{284}112$	11	SF	98^{+41}_{-23}ms		
$^{291}116$	2	α	$6.3^{+11.6}_{-2.5}$ms	20 ms	10.74±0.07
$^{287}114$	3	α	$1.1^{+1.3}_{-0.4}$s	0.5 s	10.04±0.07
$^{283}112$	3	α	$6.1^{+7.2}_{-2.2}$s	3 s	9.54±0.07
$^{279}110$	3	SF	$0.29^{+0.35}_{-0.10}$s		
$^{290}116$	2	α	15^{+26}_{-6}ms	10 ms	10.85±0.08
$^{286}114$	2	α/SF	$0.29^{+0.54}_{-0.11}$s	0.5 s	10.03±0.31
$^{282}112$	1	SF	$1.0^{+4.8}_{-0.5}$ms		

periment, we have observed three isotopes of element 114 with consecutive neutron numbers.

Based on the decay properties of nuclei in the observed decay chains and dependence of their yields on the bombarding energy, we should assign the shorter (α-SF) chain to the decay of the even-even nuclide $^{288}114$ produced via the 4*n*-evaporation channel with a maximum cross section of ~5 pb. The two different (α-α-SF) chains should be assigned to the decay of neighboring even-odd isotopes of element 114 produced in the 3*n*- and 5*n*-evaporation channels with cross sections of ~2 pb and ~1 pb, respectively. Note, in this interpretation of the data, the previously observed α decay of the parent nuclei discovered in the reactions ^{244}Pu + ^{48}Ca [1] and ^{248}Cm + ^{48}Ca [2] originated from the isotopes $^{289}114$ and $^{293}116$.

B. Synthesis of $Z=116$ nuclei in the reaction ^{245}Cm + ^{48}Ca

This experiment was designed to investigate the radioactive properties of the isotopes of element 116, the α-decay daughters of $Z=118$ isotopes produced in the reaction ^{249}Cf + ^{48}Ca [3].

The excitation energy of the compound nucleus at the Coulomb barrier of the ^{249}Cf + ^{48}Ca reaction is about 6.3 MeV lower than that of the reaction ^{244}Pu + ^{48}Ca. The maximum yield of $Z=118$ nuclides is expected in either the 2*n*- or 3*n*-evaporation channel. Similarly, the minimum excitation energy of $^{293}116$ in the ^{245}Cm + ^{48}Ca reaction is about 4.0 MeV lower than that of $^{292}114$ formed in the reaction ^{244}Pu + ^{48}Ca and thus here evaporation of two or three neutrons looks to be most probable too. Therefore, for the reaction ^{245}Cm + ^{48}Ca, we chose a lab-frame beam energy of 243 MeV in the middle of the target ($E^*=30.9-35.0$ MeV) (see Table I). At this beam energy, the production of isotopes $^{290,291}116$ is expected with high probability.

In this experiment the beam was switched off after a recoil signal was followed by an α-like signal with an energy of 9.80 MeV$\leqslant E_\alpha \leqslant$11.13 MeV in a time interval up to 4 s. The duration of the pause varied from 2 to 12 min. With an accumulated beam dose of 1.2×10^{19}, we detected five decay chains which fall into two decay types given in the fifth and fourth sections of Table II, respectively. The first type of decay represents a two- or three-step decay (ER-α-SF or ER-α-α-SF), lasting ~0.5 s. In two of the three decay chains of this type, the first α decay was not observed. The probability of detecting the preceding ER's as random events producing an accidental correlation was only about 2% in both cases. Despite the fact that the α particles were not observed in the ER-SF time interval, we tentatively assigned these events to the same ER-α-SF type, supposing that the α particles were not detected. In this experiment, we registered eight α particles by means of a detector with an 87% efficiency. Missing two α particles is not improbable. The second decay type included three sequential α decays and also ended in spontaneous fission. The total time interval between the ER and the SF for that decay type is about 10 s and is dominated by the last α decay that precedes the SF.

These new chains produced in the ^{245}Cm + ^{48}Ca experiment are different than the ER-α-α-α-SF decays of the nuclei synthesized in the reaction ^{248}Cm + ^{48}Ca [2]. Indeed, for the 10 s decay chain in the ^{245}Cm experiments, the energy of the α particles emitted by the mother and daughter nuclei ($Z=116$ and 114) are about 0.2 MeV larger and their half-lives are smaller than that observed for more neutron-rich isotopes of elements 116 and 114. An even stronger difference is observed in the decay of granddaughter nuclei ($Z=112$), where the α particle energies differ by ~0.4 MeV and the difference in half-life increases accordingly. For the 0.5 s decay chain in the ^{245}Cm experiments, the α particle energies of the mother and daughter nuclei ($Z=116$ and 114) are about 0.3 MeV and ~0.2 MeV larger and the decay modes and half-lives of granddaughter nuclei ($Z=112$) are different ($T_{SF}\sim1$ ms and $T_\alpha=34$ s, see Tables II and III).

The differences in decay properties of the daughter nuclei ($Z=114$) are also observed when comparing data from the ^{245}Cm + ^{48}Ca reaction with the short (ER-α-SF) chain that we have assigned to the decay of the even-even nuclide $^{288}114$, produced via 4*n*-evaporation in the reaction ^{244}Pu

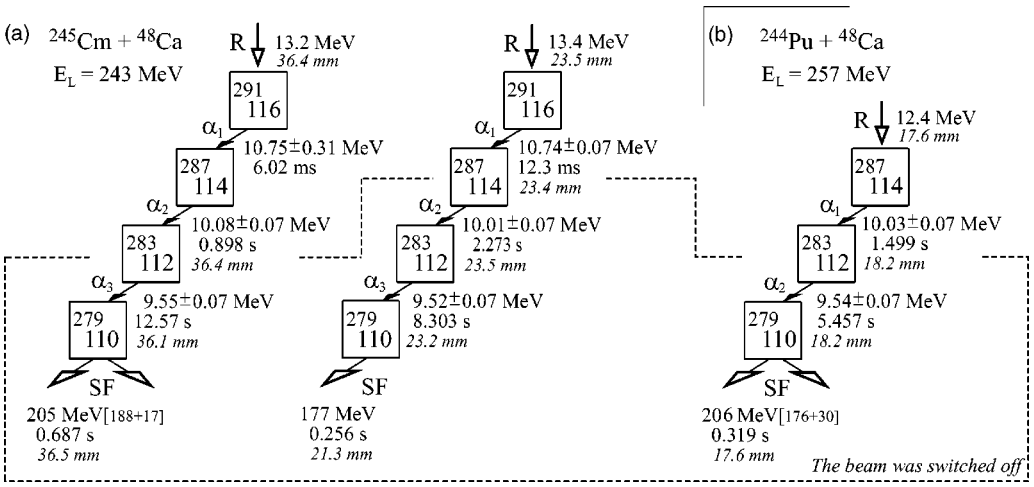

FIG. 3. Time sequences in selected decay chains observed in the ^{245}Cm+^{48}Ca (a) and ^{244}Pu+^{48}Ca (at 257 MeV) (b) reactions. Measured energies, time intervals and positions of the observed decay events are shown. Energies of SF events detected by both the focal-plane detector and side detectors are shown in brackets.

+^{48}Ca. The α decay energies of the daughters (Z=114) differ by ~0.1 MeV and the half-lives of the granddaughters (Z=112) are different. The isotope ^{284}112 decays via SF with a half-life of ~98 ms, whereas the granddaughter nucleus of the ^{245}Cm+^{48}Ca reaction products decays via α decay with a half-life of ~6 s (10 s chain) or via SF with T_{SF}~1 ms (0.5 s chain). Thus, the decay chains produced in the reaction ^{245}Cm+^{48}Ca cannot originate from ^{293}116 or ^{292}116 (0n- or 1n-evaporation channels).

However, when one compares the decay energies and half-lives of the daughter nuclei in the ER-α-α-α-SF decay chains observed in ^{245}Cm+^{48}Ca reaction with the properties of the single chain observed in the ^{244}Pu+^{48}Ca reaction at maximum beam energy (257 MeV, $E^*\approx$53 MeV), which was assigned to the decay of ^{287}114, there is excellent agreement (see Fig. 3). As a result, the longer ER-α-α-α-SF chains observed in the ^{245}Cm+^{48}Ca reaction must arise from the decay of ^{291}116 produced via the 2n-evaporation channel. Then, the shorter chains should be assigned to the decay of even-even ^{290}116, the product of 3n-evaporation. The energies of the first α decay in the short (0.5 s) and long (10 s) chains differ by just 0.1 MeV and the energies of the second α decay in both chains are close to each other. However, the correlation times of the third α decay and SF decay time in the short (ER-α-α-SF) chain differ substantially (T_α=6 s, T_{SF}=1 ms). For the daughter nucleus ^{286}114, in one decay chain we observed α decay and SF was registered in two other cases. The α decay of this isotope was not observed in the decay chain originating from ^{294}118 [3].

IV. DISCUSSION

In the present work, we measured, for the first time, the production cross sections of the ER's produced in the reaction ^{244}Pu+^{48}Ca at three ^{48}Ca beam energies: 243 MeV, 250 MeV, and 257 MeV, which correspond to the compound nucleus ^{292}114 with E^*=41.0 MeV, 46.9 MeV, and 52.6 MeV, respectively. Previous experiments [1] explored the products of this reaction at lower beam and excitation energies (E^*=31.4 MeV and 35.2 MeV).

At E^*=41 MeV and 47 MeV, three chains of sequential ER-α-α-SF decays were observed. These chains are identical to those detected in previous ^{244}Pu+^{48}Ca experiments at 236 MeV (E^*=35 MeV) and to those produced as decay products of the Z=116 nucleus observed in the ^{248}Cm +^{48}Ca reaction [2]. The maximum yield of this nuclide, ^{289}114, is observed at E^*=41 MeV with a peak production cross section of $1.7^{+2.5}_{-1.1}$ pb.

At E^*=41 MeV, 47 and 53 MeV, we observed 12 events of the decay of a new nuclide that undergoes sequential ER-α-SF decay over the span of about 1 second. The maximum yield of this nuclide, ^{288}114, corresponds to E^* $\approx$43 MeV and a peak production cross section of $5.3^{+3.6}_{-2.1}$ pb.

At the highest excitation energy of 53 MeV, another new nuclide undergoing sequential ER-α-α-SF decay was observed. The time interval between the implantation of the mother nucleus in the detector and the SF of the granddaughter isotope was about 10 seconds. The yield of this nuclide, ^{287}114, at E^*=53 MeV corresponds to a production cross section of $1.1^{+2.6}_{-0.9}$ pb.

The difference in nuclear properties expressed in the decays of daughter nuclei produced in these experiments calls for assigning the different decay chain types to different parent isotopes produced via 3n-, 4n-, and 5n-evaporation channels. From the viewpoint of decay characteristics of the Z =114 nuclei, the chains of the two ER-α-α-SF and one ER -α-SF types could be considered as both originating from the even-even nuclide ^{288}114 produced in 4n-evaporation channel. In the three different chains, the α-decay energies of the mother nuclei (Z=114) are 9.82–10.04 MeV and the half-lives are 0.63-2.7 s. These α-decay energies and half-lives are quite similar. However, the decay for the daughter nuclei (Z=112) from the three chains varies greatly. In two of the chains they undergo α decay with energies of 9.54 and 9.16 MeV with half-lives of 6 and 34 s, respectively. The daughter from the third chain decays via SF with a 98 ms half-life. These varying daughter decay properties lead to the

assignment of these three chains to three distinct mother nuclei, $^{287}114$, $^{288}114$, and $^{289}114$.

The measured excitation functions for producing of these nuclei completely corroborate such assignment. Indeed, the isotope $^{289}114$ was observed at lower excitation energies $E^*=35$ MeV, 41, and 47 MeV, the decay chains originating from $^{288}114$ were produced at higher energies, $E^*=41$ MeV, 47, and 53 MeV. The excitation functions measured for both $^{289}114$ and $^{288}114$ nuclei are characteristic in energy location, shape and magnitude of the products of neutron evaporation from the excited $^{292}114$ compound nucleus [5]. Finally, the isotope $^{287}114$ was observed only at the highest excitation energy of 53 MeV.

In the $^{245}Cm+^{48}Ca$ reaction, we synthesized two new isotopes of element 116 that undergo sequential α decays terminated by spontaneous fission. The properties of the daughter nucleus of one of the element 116 isotopes produced in the $^{245}Cm+^{48}Ca$ reaction (two events) essentially reproduces the characteristics of the 10-s (ER-α-α-SF) chain arising in the $^{244}Pu+^{48}Ca$ reaction that we assign to the decay of isotope $^{287}114$. Therefore, the longer decay chains (ER-α-α-α-SF) are assigned to the decay of $^{291}116$ produced in the $2n$-evaporation channel of the $^{245}Cm+^{48}Ca$ reaction. Then, the shorter three chains should be assigned to the decay of even-even $^{290}116$, the product of $3n$-evaporation.

The α particle spectra observed in these experiments from the decay of the nuclei with $Z=116$ and 114 are characterized by well-defined transition energies. They follow the relationship between the probability and energy of α-decay (Viola-Seaborg formula) that was determined from 65 even-even nuclei with $Z>82$ and $N>126$, for which T_α and Q_α values have been measured. This means that the observed transitions are as unhindered for the even-Z isotopes with odd mass numbers as they are for isotopes with even mass numbers. In particular, both these facts, i.e., the registration of unhindered decays and unique α-particle energies for odd isotopes produced at only one bombarding energy in our previous experiments $^{244}Pu+^{48}Ca$ (two events) [1] and $^{248}Cm+^{48}Ca$ (three events) [2] have led to their assignment to the even-even isotopes. The decay properties of nuclei produced in present experiments are given in Table III. The expected half-lives corresponding to the measured α-particle energies for the given isotopes, calculated from the Viola-Seaborg systematics, are shown in separate column behind the measured values.

The α-decay energies of the synthesized nuclei are given in Fig. 4 together with the available values of Q_α for the known isotopes with even $Z\geqslant 100$ and theoretical values [10,11]. Radioactive properties of isotopes with $Z=112$, 114, and 116 are in qualitative agreement with the macro-microscopic model calculations that predict the nuclear shapes to be close to spherical in this domain.

Despite expectations, all of the observed ER's are produced at beam energies exceeding the Coulomb barrier for the $^{244}Pu+^{48}Ca$ reaction ($B_{Bass}=233$ MeV, $E^*=32.9$ MeV). In contrast to the well-studied reactions $^{206,208}Pb+^{48}Ca$ that are used in many model calculations, the $^{244}Pu+^{48}Ca$ xn-evaporation excitation functions are shifted to higher energies. The highest yield is observed at $E^*\approx 41$ MeV, close to expectations for the $4n$-channel maximum. This points to

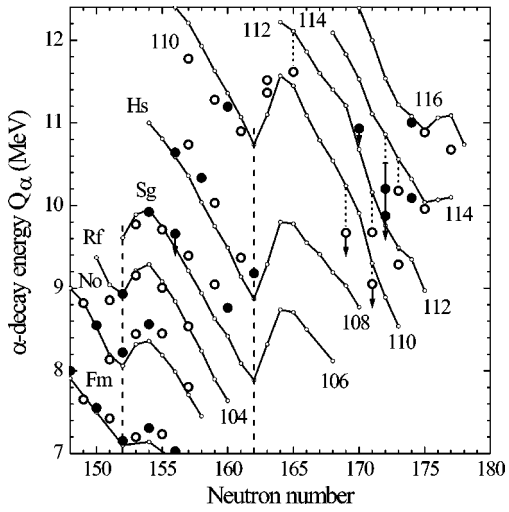

FIG. 4. α-decay energy vs neutron number for isotopes of even-Z elements with $Z\geqslant 100$ [solid circles (•), even-even isotopes; open circles (○), even-odd isotopes] [4,12,13]. Data at $N\geqslant 169$ are from [1,2] and the present work. Solid lines show theoretical Q_α values [10,11] for even $Z=100-116$ elements.

a considerable decrease in the compound nucleus formation cross-section around the Coulomb barrier. Such an effect is not observed in the fusion of Pb target nuclei with ^{48}Ca and heavier projectiles (the cold fusion reactions). This may be associated with the orientation of the deformed target nucleus during its interaction with the approaching ^{48}Ca projectile. If the major contribution to the formation of the compound nucleus is associated with the compact system in the entrance channel (the minimum distance between the centers of interacting nuclei), then as shown in [14] and in experiments with light compound nuclei [15], the fusion threshold should increase and the number of neutrons emitted from a more heated nucleus should increase accordingly.

In the $^{245}Cm+^{48}Ca$ reaction, where the mass defect decreases the minimum excitation energy of the compound nucleus $^{293}116$ by some 4 MeV compared with $^{292}114$ produced in the $^{244}Pu+^{48}Ca$ reaction, the $2n$- and $3n$-evaporation channels are observed at energies of $E^*=30.9-35.0$ MeV with cross sections of about 0.9 pb and 1.3 pb, respectively. It is evident that the problems of fusion of the deformed nuclei with massive ions like ^{48}Ca requires further experimental investigation.

Based on the measured production cross sections of new nuclides, their synthesis in the cross bombardments, as well as comparison of their decay properties with experimental systematics and theoretical predictions, it is most reasonable to assign observed nuclei to the products of the complete fusion reactions followed by neutron evaporation. For the trans-actinide compound nuclei, the αxn or pxn reactions were not previously observed in the reactions induced by heavy projectiles with $A\geqslant 40$ (see, e.g., [4,16] and references therein). From our experiments $^{206}Pb(^{48}Ca,1\text{-}4n)^{250-253}No$ [17] we set the upper cross section limits for the ($\alpha 2n+a3n$) reactions to be lower by a factor of 33 than that of the $2n$ evaporation channel at its maximum and by factors of 6 and 3 at $E^*=20$ MeV and 40 MeV, respectively. Moreover,

the separator transmission for such reaction products is about an order of magnitude lower compared with the products of *xn* evaporation. Besides, the assignment of the new synthesized nuclei to the αxn- or p*xn*-reaction products would result in noticeable excess of experimental Q_α values over the theoretical ones and in considerable deviations from the experimental T_α vs. Q_α systematics.

From the theoretical consideration, the ^{48}Ca-induced reactions with actinide nuclei essentially differ from the cold-fusion one. In the latter case, the production of residual nuclei is largely determined by the decrease of compound nucleus formation probability with increasing of projectile mass thus resulting in gradual reduction of their yields. For the more asymmetrical ^{48}Ca-induced reactions with actinide targets, the probability of compound nucleus formation is substantially higher but the yields of ER's largely depend on their survival probability during the deexcitation of hot nuclei. The recent calculations [9] well reproduce the measured cross sections for the reactions of ^{244}Pu, ^{243}Am [18], ^{245,248}Cm [2], and ^{249}Cf [3] with ^{48}Ca. However, the calculations of cross sections for the production of superheavy nuclei in these reactions are rather complex and uncertain because of lack of adequate microscopic model for description of compound nucleus formation process and precise parameters of such nuclei, for instance their fission barriers, nucleon separation energies, and nuclear deformation parameters. In this respect, further experiments aimed at the investigations of chemical properties and precise mass measurements of descendant nuclei in the observed decay chains as well as synthesis of heavy nuclei decaying to the known nuclides in the ^{48}Ca induced reactions with actinide targets are highly desirable.

In view of these interpretations, the data of our first experiments [19] performed at low excitation energies ($E^* \leqslant 35$ MeV) need further analysis. In the present ^{244}Pu $+^{48}$Ca experiment, at $E^* = 41$ MeV, 47 and 53 MeV and a total beam dose of 1.0×10^{19} as well as in the previous experiment [1] at $E^* = 35$ MeV with a beam dose 1.0×10^{19}, we did not observe the long decay chain similar to that which we had detected in our first experiment [19] at $E^* = 35$ MeV, which we interpreted as a *candidate* for the decay of ^{289}114. The cross section corresponding to this single event was estimated to be about 0.2 pb at $E^* = 35$ MeV. In view of the recent results, one could propose that this chain originates from the decay of the neighboring isotope ^{290}114 produced via 2*n*-evaporation. Indeed, the energy of the first α particle (9.71 MeV) is about 0.1 MeV lower than that of the isotope ^{289}114 assigned from our most recent work, and the energies of the next two α particles (8.67 MeV and 8.83 MeV) do not contradict what is expected for ^{286}112 and ^{282}110. Yet in this case, one has to suppose a considerable increase in stability against decay by SF of ^{286}112 compared with its lighter even-even neighbor ^{284}112 ($T_{SF} \approx 0.1$ s).

On the other hand, some calculations [20] show that such a long chain can be assigned to a rare decay branch of the even-odd nuclide ^{289}114. This rare decay starts from the isomeric first excited state rather than from the ground state, and goes through low-lying levels in the daughter nuclei in accordance with the selection rules associated with the appropriate quantum numbers.

In the present experiments, we did not observe the 3 or 5 min ER-α-SF decay chain reported in the ^{242}Pu$+^{48}$Ca reaction studied with the VASSILISSA separator and assigned to ^{287}114 [21]. In order to resolve the remaining contradictions concerning properties of ^{287}114 and ^{283}112 we plan to study excitation functions for their production in the reactions ^{242}Pu$+^{48}$Ca and ^{238}U$+^{48}$Ca in the nearest future.

ACKNOWLEDGMENTS

This work has been performed with the support of the Russian Ministry of Atomic Energy and grants of RFBR, Nos. 01-02-16486, 03-02-06236 and 04-02-17186. The ^{244}Pu target material was provided by the U.S. DOE through ORNL. The ^{245}Cm target material was provided by RFNC-VNIIEF, Sarov. Much of the support for the LLNL authors was provided through the U.S. DOE under Contract No. W-7405-Eng-48. The LLNL authors would like to thank their Russian co-authors for hosting them during their visits to participate in the ^{244}Pu$+^{48}$Ca and ^{245}Cm$+^{48}$Ca experiments, and for the lively discussions regarding the interpretation of the data. These studies were performed in the framework of the Russian Federation/U.S. Joint Coordinating Committee for Research on Fundamental Properties of Matter.

[1] Yu. Ts. Oganessian *et al.*, Phys. Rev. C **62**, 041604(R) (2000); Phys. At. Nucl. **63**, 1679 (2000).

[2] Yu. Ts. Oganessian *et al.*, Phys. Rev. C **63**, 011301(R) (2001); Phys. At. Nucl. **64**, 1349 (2001); Eur. Phys. J. A **15**, 201 (2002).

[3] Yu. Ts. Oganessian *et al.*, JINR Communication D7-2002-287, 2002; Lawrence Livermore National Laboratory Report, UCRL-ID-151619, 2003.

[4] S. Hofmann and G. Münzenberg, Rev. Mod. Phys. **72**, 733 (2000); S. Hofmann *et al.*, Eur. Phys. J. A **14**, 147 (2002).

[5] R. C. Barber *et al.*, Prog. Part. Nucl. Phys. **29**, 453 (1992).

[6] Yu. Ts. Oganessian *et al.*, *Proceedings of the Fourth International Conference on Dynamical Aspects of Nuclear Fission*, Častá-Papiernička, Slovak Republic, 1998 (World Scientific, Singapore, 2000), p. 334; K. Subotic *et al.*, Nucl. Instrum. Methods Phys. Res. A **481**, 71 (2002).

[7] W. D. Myers and W. J. Swiatecki, Nucl. Phys. **A601**, 141 (1996).

[8] R. Bass, *Proceedings of the Symposium on Deep Inelastic and Fusion Reactions with Heavy Ions*, West Berlin, 1979, edited by W. von Oertzen, Lecture Notes in Physics Vol. 117 (Springer-Verlag, Berlin, 1980), p. 281.

[9] V. I. Zagrebaev, M. G. Itkis, and Yu. Ts. Oganessian, Phys. At. Nucl. **66**, 1033 (2003); V. I. Zagrebaev *et al.*, Nucl. Phys. **A734**, 164c (2004).

[10] R. Smolańczuk and A. Sobiczewski, *Proceedings of XV*

Nuclear Physics Divisional Conference "Low Energy Nuclear Dynamics," St. Petersburg, Russia (World Scientific, Singapore, 1995), p. 313.
[11] I. Muntian *et al.*, Acta Phys. Pol. B **34**, 2073 (2003); Phys. At. Nucl. **66**, 1015 (2003).
[12] Ch. E. Düllmann *et al.*, Nature (London) **418**, 859 (2002).
[13] *Table of Isotopes*, 8th ed., edited by R. B. Firestone and V. S. Shirley (Wiley, New York, 1996).
[14] P. Möller and J. R. Nix, *Proceedings of the Tours Symposium on Nuclear Physics III*, Tours, France, 1997, edited by M. Arnould, M. Lewitowicz, Yu. Ts. Oganessian, M. Ohta, H. Utsunomiya, and I. Wada, AIP Conf. Proc. No. 425 (AIP, New York, 1998), p. 75.
[15] K. Nishio *et al.*, J. Nucl Sci. Tech., Supplement 3, *Proceedings of the Actinides 2001 International Conference*, Hayama, Japan, 2001 (Atomic Energy Society of Japan, 2002), p. 26.
[16] Yu. Ts. Oganessian *et al.*, Radiochim. Acta **37**, 113 (1984); Yu. A. Lazarev *et al.*, Nucl. Phys. **A580**, 113 (1994).
[17] Yu. Ts. Oganessian *et al.*, Phys. Rev. C **64**, 054606 (2001).
[18] Yu. Ts. Oganessian *et al.*, Phys. Rev. C **69**, 021601(R) (2004).
[19] Yu. Ts. Oganessian *et al.*, Phys. Rev. Lett. **83**, 3154 (1999).
[20] S. Ćwiok, W. Nazarewicz, and P. H. Heenen, Phys. Rev. Lett. **83**, 1108 (1999); J. F. Berger, D. Hirata, and M. Girod, Acta Phys. Pol. B **34**, 1909 (2003).
[21] Yu. Ts. Oganessian *et al.*, Nature (London) **400**, 242 (1999); Eur. Phys. J. A **5**, 63 (1999); **19**, 3 (2004).